DFI-EFFC International Conference on Deep Foundations and Ground Improvement:
Urbanization and Infrastructure Development-Future Challenges
June 06, 2018 - June 08, 2018
Sapienza University, Rome, Italy

A study of the augmenting effect of equipping piles with an Expander Body

Bengt H. Fellenius[1)], K. Rainer Massarsch[2)], and Mario Terceros H.[3)]

[1)]Consulting Engineer, 2475 Sidney, BC, Canada, V8L 2B9. <Bengt@fellnius.net>
[2)]Geo Risk & Vibration AB, Bromma, Sweden. <rainer.massarsch@georisk.se>
[3)]Incotec S.A., Santa Cruz de la Sierra, Bolivia <mta@incotec.cc>

ABSTRACT. A full-scale study is reported of the response of eight piles in four pairs: a 150 mm diameter gravity-grouted micro-pile pile, a 600-mm diameter bored pile drilled with slurry, a 450 mm diameter continuing-flight auger-cast pile (CFA), and a 450 mm diameter, full-displacement pile (FDP). One of each pair was equipped with an Expander Body to increase the pile-toe diameter, preload the pile axially, as well as bring about a stiffer pile toe and, thus, achieve a stiffer pile. All piles were constructed to 9.5 m depth in a loose to dense silty to dense sand at the ISSMGE research site in Santa Cruz Bolivia. The EB-equipped piles were supplied with bidirectional cell immediately above the EB (depth 8.3 m). Static loading tests performed on all piles showed that the expansion of the EB markedly increased the pile toe stiffness. This, not just by increasing the pile toe area, but also by preloading the soil underneath the pile toe and increasing the shaft resistance acting around the 1.5 m long EB. Moreover, the test results indicated that the EB expansion also built in residual load in the pile which resulted in a stiffer shaft response.

KEYWORDS. Bored, CFA, and Full Displacement piles, static loading test, pile-toe augment.

INTRODUCTION

The pile testing programme at the ISSMGE research site in Santa Cruz, the Bolivian Experimental Site for Testing Piles (B.E.S.T.) was organized in conjunction with the 3rd International Conference on Deep Foundations, April 27 – 29, 2017, in Santa Cruz de la Sierra, Bolivia. The programme included static loading tests on piles with and without a toe augment, an expandable device (Expander Body, EB), to increase the pile toe area and to improve the pile toe resistance. Four types of piles were constructed in pairs to 9.5 m depth in a silty to dense sand**:** (1-Piles D) a 150 mm diameter gravity-grouted micro-pile pile, (2-Piles A) a 620-mm diameter piles drilled with slurry, (3-Piles B) a 450-mm diameter continuous flight auger pile, and (4-Piles C) a 450-mm diameter full displacement pile. Each pair had one pile with an EB and one without.

A head-down static loading test was carried out on the piles without an EB. The four EB-piles, were tested using a bidirectional test.

The purpose of the here reported tests was to compare the static response of piles with and without an EB. The details of the piles, testing programme, and test results are presented.

SOIL PROFILE

The site investigation at the B.E.S.T. site, the soil exploration, notably the CPTU sounding results, show the soil profile to consist of essentially two soil layers: an upper 6 m thick layer of loose silt and sand on compact silty sand. The CPTU pore pressure measurements indicated a groundwater table at or near about 0.5-m depth and a hydrostatically distributed pore pressure. Figure 1 shows a diagram compiling the SPT N-indices and the CPTU cone stress, q_t. For additional in-situ test results, including pressuremeter and dilatometer tests, see the conference website: http://www.cfpbolivia.com/web/page.aspx?refid=157.

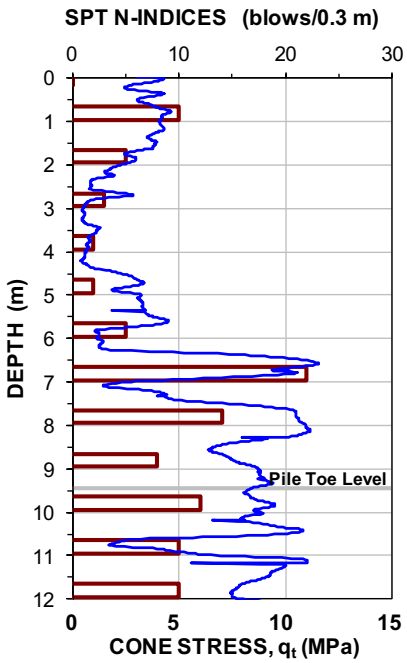

Fig. 1. SPT N-indices compiled with the CPTU q_t-stress at Pile A3.

THE EXPANDER BODY (EB)

The EB is a 1 to 2 m long folded, 120 mm wide steel tube that is expanded (inflated) by pressure-grouting delivered through a grouting tube placed in the reinforcing cage (Figure 2). Different models allow for expansion to 400 through 800 mm diameter width. Pressure and volume of the grout during the expansion of the Expander Body are continuously recorded. The lateral expansion of the EB causes the length of the EB tube to shorten by about 100 mm, manifested as a lifting of the EB bottom-end or pull-down of the shaft in loose or soft soil. As the EB is connected to the pile reinforcing cage, the expansion imposes some tension in the pile. Any soil decompression created below the expanded EB is offset by a second-phase grouting of the soil at the pile toe. Maximum grouting pressure below the EB is typically of the same magnitude as the BE-expansion pressure, for the current piles it was about 1.0 through 2.5 MPa. The toe grout is delivered through a separate grout tube inside the grout tube and passing through the EB. In-air tests have shown that about 100 kPa pressure is needed to expand the EB.

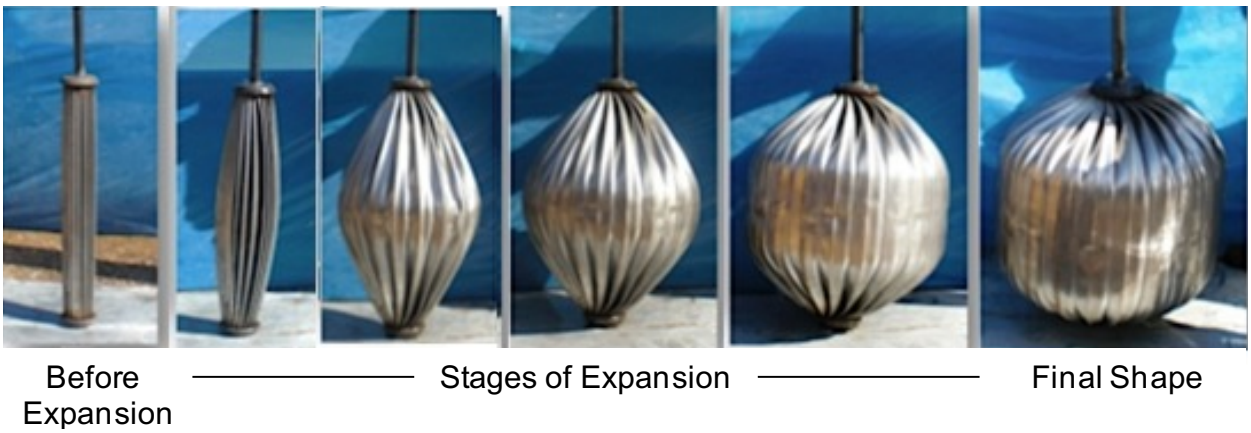

Fig. 2. In-air demonstration of EB expansion.

Figure 3 shows a sketch of the pile and EB arrangement at the B.E.S.T. site. The EB original length was 1.20 m and a bidirectional cell (hydraulic jack) jack, 300 mm high by 220 mm wide, was connected to the top of the EB and reinforcing cage.

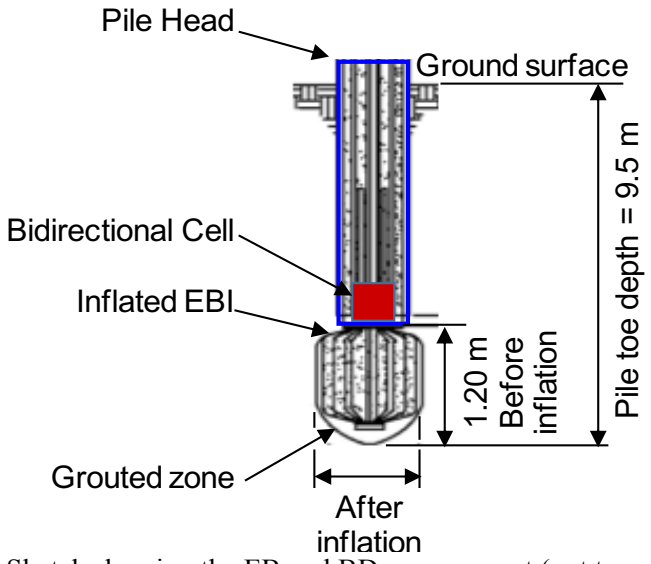

Fig. 3. Sketch showing the EB and BD arrangement (not to scale).

TEST PILES

The details of the test piles are listed in Table 1.

TABLE 1 Pile description

Type		BD EB	Final EB Volume (L)	Final Pressure (MPa)	Estimated EB and TB width (mm)	Shaft Grouting Method
150-mm micro pile	D1	EB	130	1.1	400	Gravity
150-mm micro pile	D2	- - -				Gravity
450 mm CFA pile	B1	BD+EB	200	1.0	500	Pressure
450 mm CFA pile	B2	- - -				Pressure
620 mm Bored Pile	A1	BD+EB	245	2.3	600	Gravity
620 mm Bored Pile	A3	- - -				Gravity
450 mm FDP pile	C1	BD+EB	210	2.0	500	Pressure
450 mm FDP pile	C2	- - -				Pressure

BD = bidirectional jack, EB = Expander Body with post-grouting below EB (maximum pressure: 2.5 MPa).

TEST RESULTS

The static loading tests, bidirectional (BD) and head-down (HD) tests, were carried out by applying equal increments of load holding the load level constant for ten minutes. Tests on piles with BD jack and EB device started with the BD test followed by the HD test. In each static loading test—bidirectional as well as head-down—the applied load and movement along with readings of strain at three strain-gage levels (2.0, 5.0 and 7.5 m depth) were recorded.

Bored piles, Piles D and A, comparison of head-down test results

Piles D1 and D2 were 150-mm diameter, 9.5 m long, bored with slurry, gravity-grouted micro piles with a nominally 0.0177 m^2 cross section area. Piles A1 and A3 are : 620-mm diameter, 9.5 m long, bored with slurry, gravity-grouted piles with a nominally 0.3019 m^2 cross section area. Piles D1 and A1 were equipped with an EB at 8.3 m depth, while Piles D2 and A3 had no such augment. Strain values between the construction of the piles and start of the test were not recorded. Pile A1 was tested using a bidirectional cell placed immediately above the EB. In Pile D2, the strains recorded during the tests were small and erratic. In contrast, the strain records in Pile A3 were consistent. Due to small strains and residual force induced in expanding the EB, the strain records in Piles D1 and A1 are of limited value.

Figure 4A shows the pile-head load-movement curve and the load distribution of the test on Pile D2. After assessing the load-movement curve, a "target point" (144 kN load at 15 mm movement), on the curve was chosen and the target load was matched in an effective stress analysis by way of effective stress proportionality coefficients (ß) for the shaft and a toe resistance. For the 0 to 6.0 m soil layer consisting of loose silt and sand ß = 0.40 was used. For the 6.0 to 9.5 m layer consisting of compact silty sand, a ß = 0.60 was used. (N.B., the shear resistance does not occur as slippage, but as shear within a band of soil of small, but unknown, thickness). For Pile D2, a unit pile toe stress, r_t, equal to 1.0 MPa, was used in the fit to the target point (at a 13-mm pile toe target movement). The analysis, using the UniPile software (Goudreault and Fellenius 2014), then continued by trying out different t-z and q-z functions, assuming and adjusting the function coefficients for the shaft and toe resistances until obtaining a simulated load-movement curve that fitted the measured curve. The adjustments were for the shape of the t-z and q-z curves, the resistance values that gave the fit to the at target point were not changed. (Background and mathematics of the t-z/q-z functions are presented in Fellenius 2016; 2018). The so-simulated pile-head, pile-toe, and pile-compression curves are shown along with the measured Pile D2 load-movement curve.

Figure 4B shows the Pile D2 simulated load distribution for the target load. The strain-gage values were too small and erratic for meaningful evaluation. The load-distribution graph is supplemented with the CPTU q_t-distribution and the load-movement curve with the target point indicated.

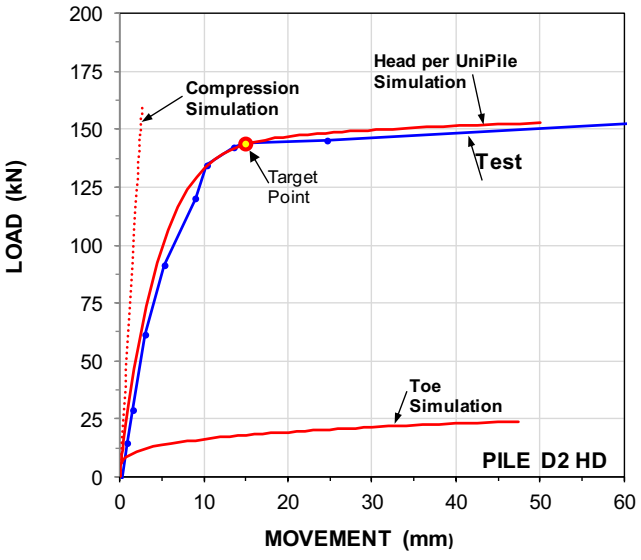

Fig. 4A Pile D2 load-movement curves

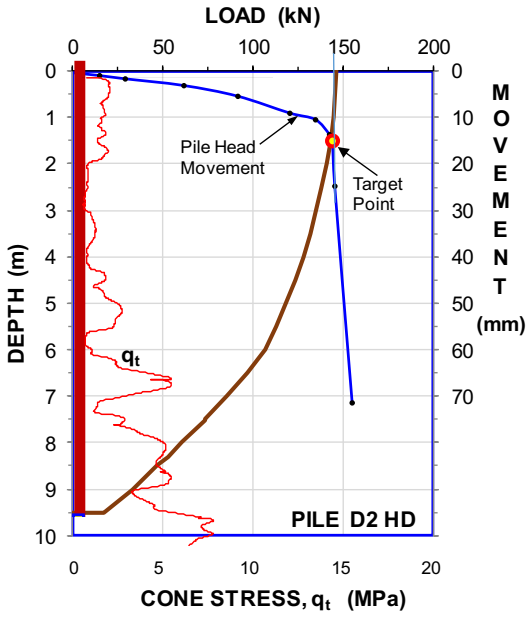

Fig. 4B Pile D2 load distribution .

Figure 5A shows the Pile A3 pile-head load-movement curve and Figure 5B shows the simulated load distribution for the Pile A3 target load and includes also the distribution determined from the strain-gage values. The target load was 835 kN load at 30 mm movement.

The target point for Pile A3 was chosen because it was produced with the same beta-coefficients and the same target toe stress as used for the analysis of Pile D2. Note, however, that the movement necessary for the coincidence of the beta-coefficients and the pile toe unit stress, was precisely twice for the analysis of the Pile A3 records as for the Pile D2 records. Pile A3 has a four times larger diameter and a 16 times larger toe area.

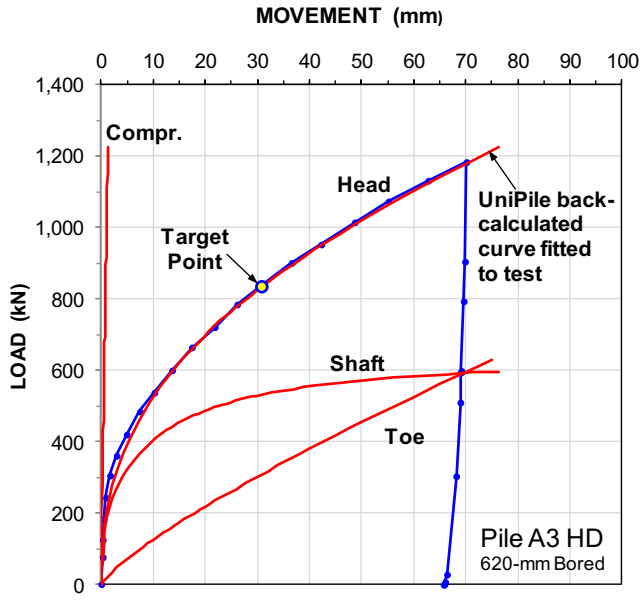

Fig. 5A Pile A3 load-movement curves

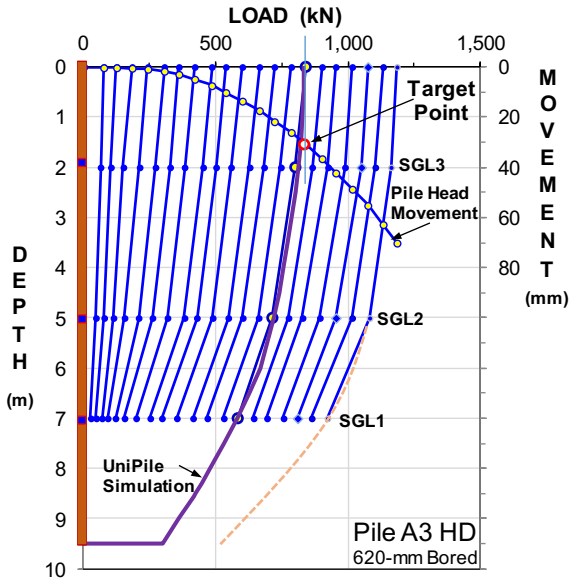

Fig. 5B Pile A3 load distribution

Figure 6 and 7 show the shaft resistance functions used to obtain the load-movement fit for Piles D2 and A3. Figure 8 shows the toe resistance functions. The "δ" indicates the movement for the target point and the "100 %" indicates the target resistance for the soil-pile elements.

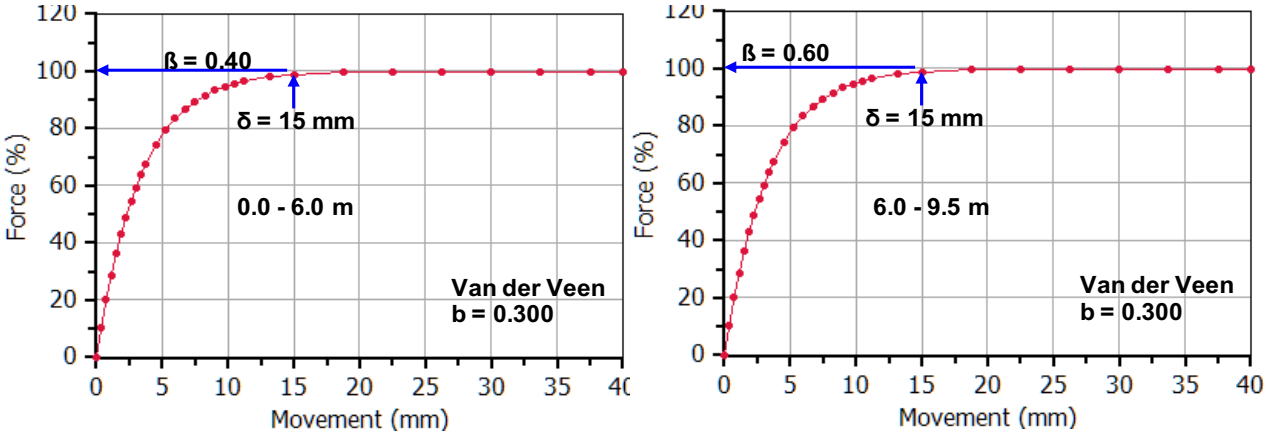

Fig. 6. Pile D2 t-z functions for the fit to the pile head load-movement curve.

Figure 9A shows the simulated test curves load-movement curve of Pile D1 (identical to Pile D2, but for the EB at the toe of Pile D1, where the nominal EB-diameter was input). Figure 9B shows the Pile D1 load-distributions. The target point matched in the analysis was 550 kN load at 7 mm movement. The test records, notably, the strain-gage records, indicated that residual force had developed in the pile before the static loading test, but they were not consistent enough to warrant analysis. The dashed set of pile-head and

toe load-movement curves in the figure are a speculative set of load-movement curves for the test had it been unaffected by residual force. (The procedure and decisions for establishing the distribution unaffected by residual force is beyond the scope of this paper).

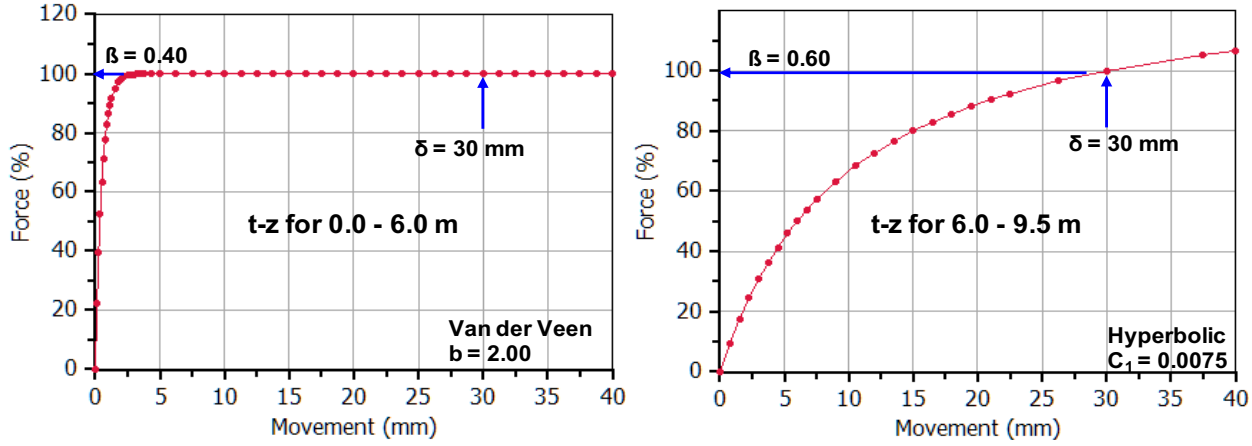

Fig. 7. Pile A3 t-z functions for the fit to the pile head load-movement curve

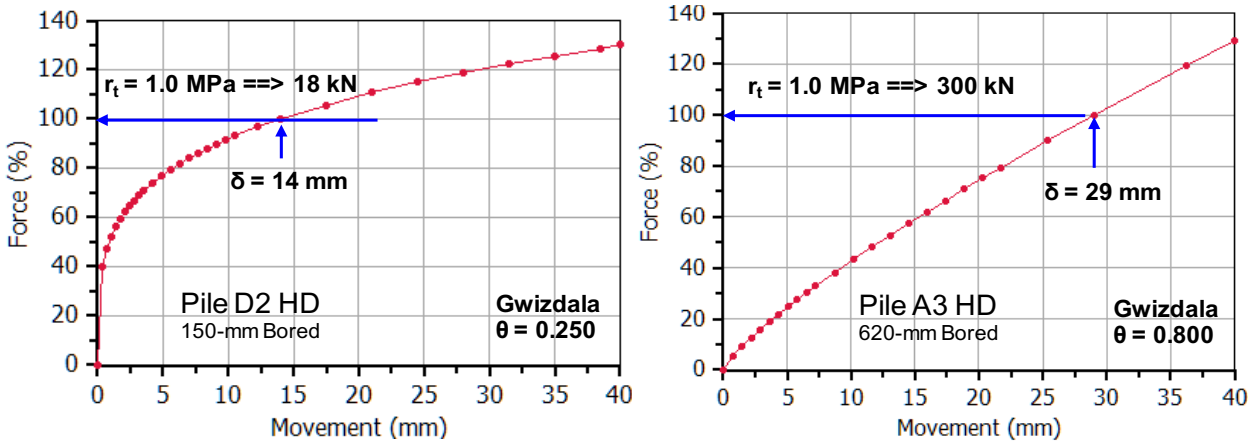

Fig. 8. Pile D2 and Pile A3 q-z functions for the fit to the pile head load-movement curve

Similarly, Figure 10A shows the simulated bidirectional-test load-movement curve of Pile A1 (Pile A1 is identical to Pile A3, but for the EB at the pile toe). Figure 10B shows the Pile A1 simulated load distribution for the target load and includes also the calculated equivalent head-down load distribution. The target load was 835 kN load at 30 mm movement. The strain-gage at 2.0 m depth did not function and the strain recorded by the gages at 5.0 m and 7.5 m depth were too small (<40 με) to allow conversion to load. However, the bidirectional test provides the benefit that the load applied and measured by the bidirectional device (hydraulic jack) is the true load. That is, it includes any potential residual force, unlike strain-gage instrumentation, which always requires consideration of adjustment to potential residual force in the pile. Thus, the "Target Point bidirectional load" is a true load.

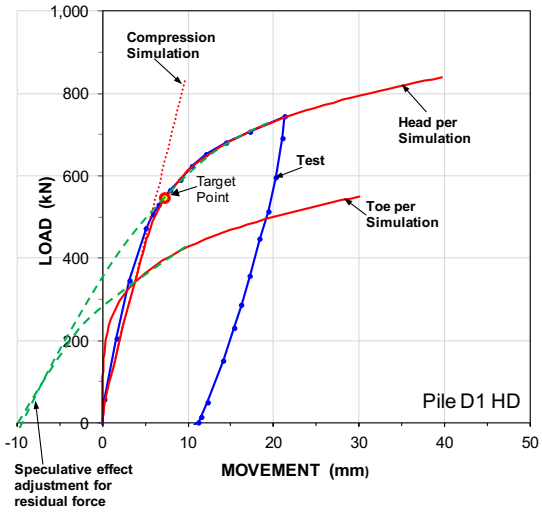

Fig. 9A. Pile D1 load-movement curves.

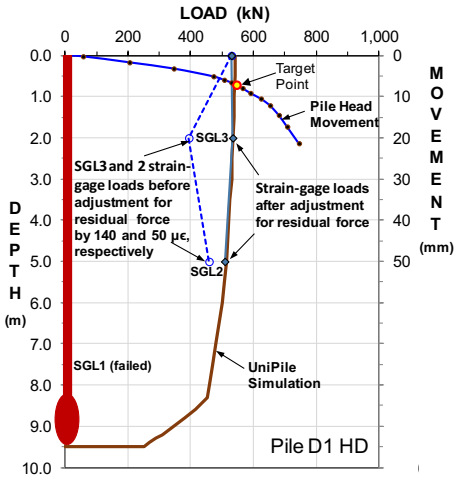

Fig. 9B. Pile D1 load distribution.

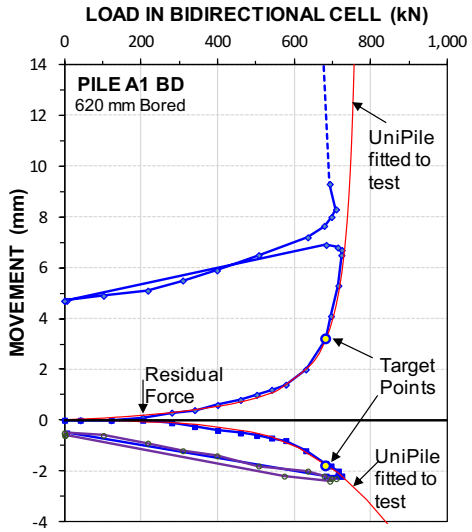

Fig. 10A. Pile A1 load-movement curves.

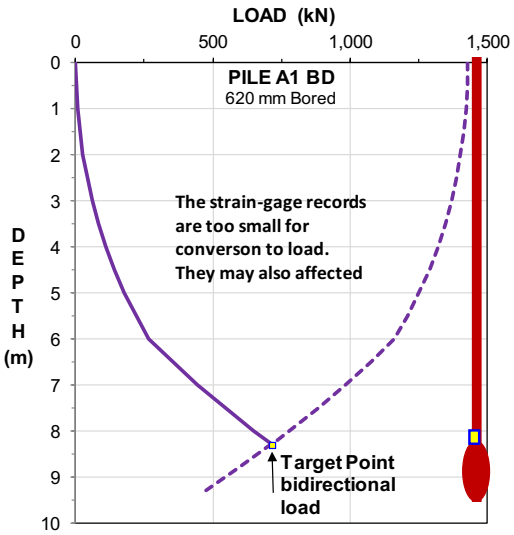

Fig. 10B. Pile A1 load distribution.

Bored piles, Piles D and A, compared with and without EB

For the micro piles, Piles D1 and D2, the beta-coefficients above the EB level (8.3 m) are equal. Below this depth, i.e., along the EB, the Pile D1 simulation fit showed ß = 1.50, i.e., more than twice that for Pile D2 along the same depth. The fitted unit toe resistance for Pile D1 was 2.0 MPa at 1 mm movement (corresponding to 3.8 MPa at 14 mm) as opposed to 1.0 MPa for Pile D2 at 14 mm movement. The t-z and q-z function produced in the fitting show that the EB has not just provided a larger resistance, it has also stiffened up the response of the pile to the applied load.

The load-movement curves and load distributions for the two bored with slurry, gravity-grouted D-piles are compared in Figures 12A and 12B. The pile-head load-movement curves show that equipping the micro pile with the EB increased the total pile resistance about four times. No change in shaft resistance occurred above 8.3 m depth, while the resistance below 8.3 m depth, the EB zone, increased from 50 kN to 450 kN. Below 8.3 m depth, the unit shaft resistance along the EB and the unit toe resistance was more than about twice that of the pile with no EB.

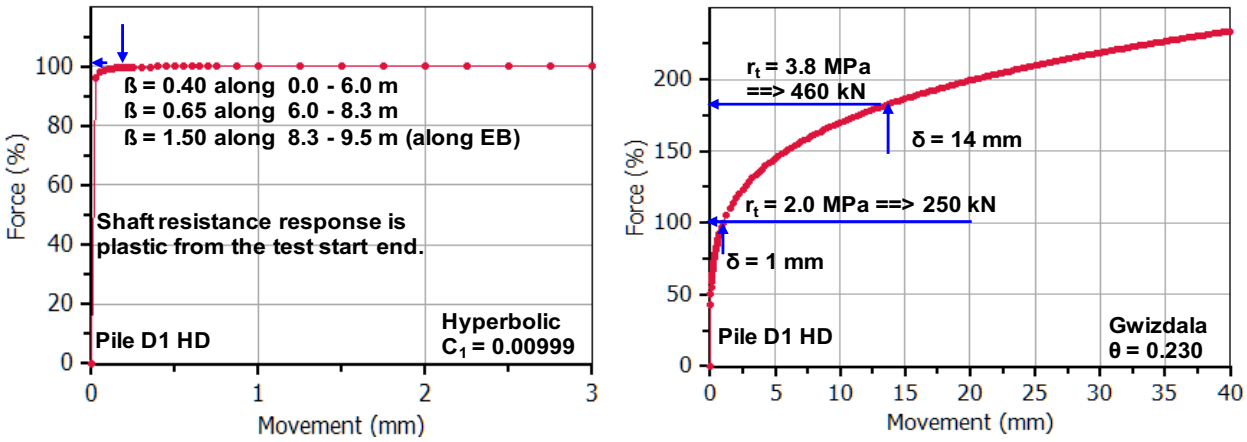

Fig. 11. Pile D1 t-z and q-z functions for the fit of the EB response.

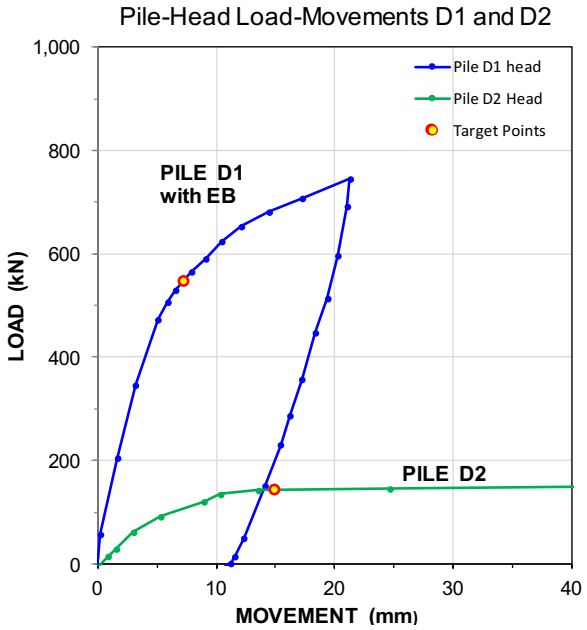

Fig. 12A. Piles D1 and D2 load-movement curves

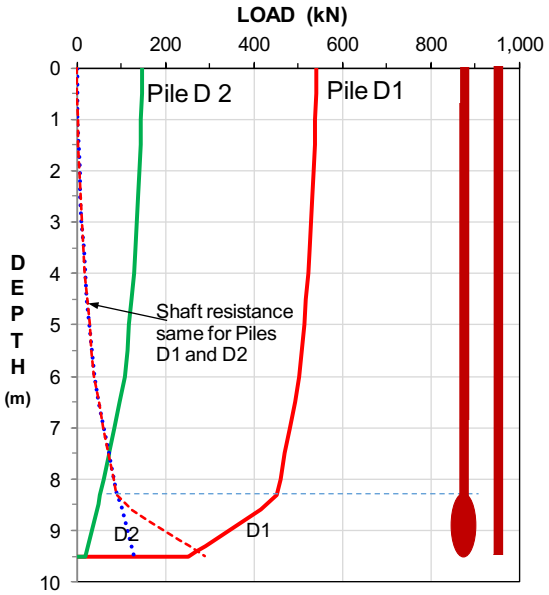

Fig. 12B. Piles D1 and D2 load distribution

For the 600-mm diameter bored piles, Piles A1 and A3, Figure 13A shows the Pile A1 actual downward test and the simulated downward test for Pile A3 calculated using UniPile from the conditions for the simulation by the head-down test. Similarly, Figure 13B show the Equivalent head-down test calculated from the simulation of the bidirectional test and the actual head-down test on Pile A3. Again, the comparison shows that the response of the EB-equipped pile was considerably stiffer than that of the straight, unaugmented pile. If the acceptable limit would be 5 to 10 mm movement (settlement) for an applied load, the EB-equipped pile would support about three times higher load than the straight pile for both bored piles, the micro pile and the 0.6-m diameter pile.

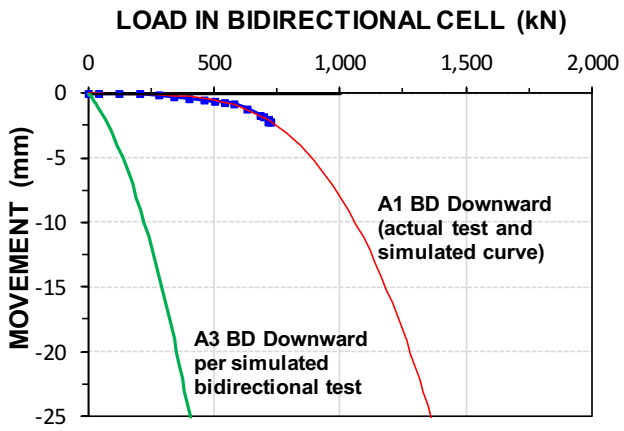

Fig. 13A. Piles A1 and A3 downward curves for a BD at 8.3 m depth.

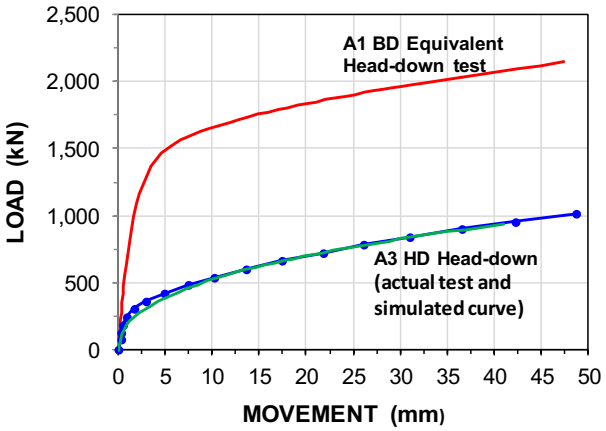

Fig. 13B. Piles A1 and A3 pile-head load-movements.

CFA piles, Piles B1 and B2, with and without EB comparison

Piles B1 and B2 were 450-mm diameter, 9.5 m long, pressure-grouted CFA piles with a nominally 0.1590 m^2 cross section area. Pile B1 was equipped with an EB at 8.3 m depth, while Pile B2 was straight. Pile B1 was tested using a bidirectional cell placed immediately above the EB. Unfortunately, the telltale measuring the downward movement of the EB (the EB was the base of the bidirectional test) of Pile B1 test failed. That is, the test records only include the upward movements and the BD loads.

Piles B test records were analyzed similarly to the procedure used for the bored piles, Piles D and A, and showed that the unit shaft resistance along the CFA-constructed piles was stiffer than for the bored piles. In order to save space, the factual load-movement , load-distribution, and simulation results are not presented here. The can be examined at: http://www.cfpbolivia.com/web/page.aspx?refid=157. Figure14A compares the bidirectional downward curve of Pile B1 (movement measurement failed) to the similar curve simulated from the results of the head-down test on Pile B2calculated using UniPile. Similarly, Figure 14B shows the actual and simulated load-movement curves of the head-down test on Pile B2 and the equivalent head-down curve calculated from the simulation of the bidirectional test. Again, the comparison shows that the response of the EB-equipped pile, Pile B1, was considerably stiffer than that of the straight, unaugmented pile, Pile B2. If the acceptable limit would be 5 to 10 mm movement (settlement) for an applied load, the EB-equipped CFA-pile would support about a twice higher load than the straight pile.

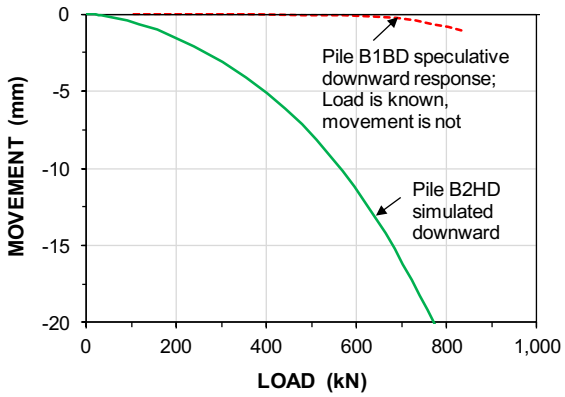

Fig. 14A. Piles B1 and B2 downward curves for a BD at 8.3 m depth.

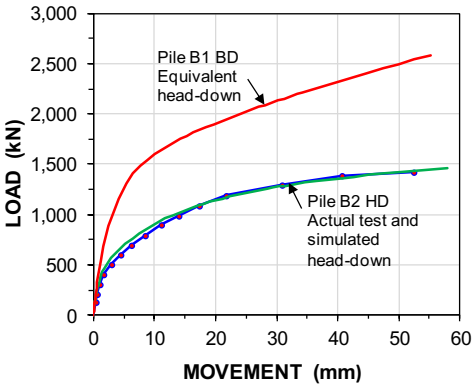

Fig. 14B. Piles B1 and B2 pile-head load-movements.

FDP piles, Piles C1 and C2, with and without EB comparison

Piles C1 and C2 were 450-mm diameter, 9.5 m long, pressure-grouted, full-displacement (FDP) piles with a nominally 0.1590 m^2 cross section area. Pile C1 was equipped with an EB at 8.3 m depth, while Pile C2 was straight. Pile C1 was tested using a bidirectional cell placed immediately above the EB. Unfortunately, the records of the BD tests were lost. A head-down reloading test was carried out after first closing the 12-mm opening in the BD jack produced in the BD test. Again, in order to save space, the factual load-movement, load-distribution, and simulation results are not presented here. The results are available at: http://www.cfpbolivia.com/web/page.aspx?refid=157.

The analysis of Piles C test records showed that the unit shaft resistance was stiffer than for the bored piles. Figure 15 shows the load-movement curve of the head-down test on Pile C2 and the equivalent head-down curve calculated from the simulation of the bidirectional test. As was the case for Piles B, the comparison shows that the response of the EB-equipped Pile C1 was considerably stiffer than that of the straight, unaugmented Pile C2. If the acceptable limit would be 5 to 10 movement (settlement) for an applied load, the EB-equipped CFA-pile would support about an about 30 % higher load than the straight pile.

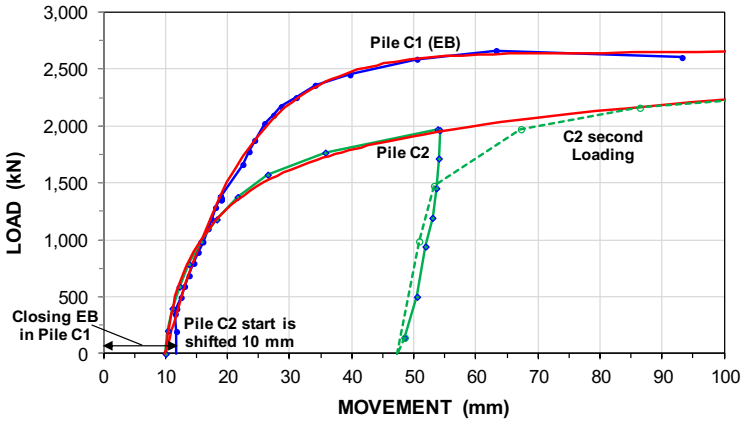

Fig. 15. Piles C1 and C2 pile-head load-movement curves.

CONCLUSIONS

For all four piles types, equipping the pile toe with the EB with post-installation grouting considerably increased the pile stiffness response to applied load. The improvement was largest for the bored pile and smaller for the CFA and the FDP piles as the construction method of these piles improve the pile shaft resistance making the relative improvement of the toe resistance less pronounced.

The expansion of the EB resulted in imposing axial residual force in the piles further enhancing the pile stiffness.

References

Fellenius, B.H., 2016. An Excel template cribsheet for use with UniPile and UniSettle. www.Fellenius.net.

Fellenius, B.H., 2018. Basics of foundation design–a textbook. Pile Buck International, Inc., Vero Beach, FL, Electronic Edition, www.Fellenius.net, 468 p.

Goudreault, P.A. and Fellenius, B.H., 2014. UniPile Version 5, User and Examples Manual. UniSoft Geotechnical Solutions Ltd. [www.UniSoftGS.com]. 120 p.

Terceros, M.H. and Massarsch, K.M, 2014. The use of the expander body with cast in-situ piles in sandy soils. Proceedings of the DFI-EFFC International Conference on Piling and Deep Foundations, Stockholm, May 21-23, pp. 347-358.